

ARTICLE

Quantitative Immunogold Labeling of Bone Sialoprotein and Osteopontin in Methylmethacrylate-embedded Rat Bone

O. Laboux, L-G. Ste-Marie, F.H. Glorieux, and A. Nanci

Laboratory for the Study of Calcified Tissues and Biomaterials, Faculty of Dentistry, Université de Montréal, Québec, Canada (OL,AN); Metabolic Bone Diseases Laboratory, Centre de Recherche du CHUM, Hôpital St Luc, Montréal, Québec, Canada (L-GS-M); Genetics Unit, Shriners Hospital for Children, and Department of Surgery and Human Genetics, McGill University, Montreal, Québec, Canada (FHG); and INSERM E.M.I., Nantes, France (OL).

SUMMARY Methylmethacrylate (MMA) embedding of undecalcified bone is routinely employed for histomorphometric analyses. Although MMA-embedded bone has been used for immunolabeling at the light microscopic level after removal of the resin, there are no such reports for electron microscopy. The aim of the present study was to determine whether MMA embedding can be used for ultrastructural immunolabeling and how it compares to LR White (LRW), an acrylic resin frequently used for immunocytochemistry of bone. Rat tibiae were fixed by vascular perfusion with aldehyde and embedded either in MMA or LRW resin. Thin sections were processed for postembedding protein A–gold immunolabeling with antibodies to rat bone sialoprotein (BSP) and osteopontin (OPN). The density of gold particles over bone was quantified. The density and distribution of immunolabeling for BSP and OPN respectively, were comparable between MMA and LRW. These results indicate that MMA performs as well as LRW for the ultrastructural immunolabeling of noncollagenous bone matrix proteins. (*J Histochem Cytochem* 51:61–67, 2003)

KEY WORDS

bone
bone sialoprotein
immunocytochemistry
LR White resin
methylmethacrylate
osteopontin

ACRYLIC RESINS are widely used for immunolabeling because they permit a good balance between tissue preservation and retention of antigenicity. Among them, methylmethacrylate (MMA) offers a number of advantages. Tissue penetration is good, a particularly important property for larger specimens and calcified tissue samples. MMA can be removed easily and completely from tissue sections, resulting in superior staining characteristics and good morphological detail (Erben 1997; Derkx et al. 1998). It is also compatible with various fluorochromes administered in vivo for dynamic histomorphometric studies of bone (Gruber et al. 1985). These characteristics have favored the use of MMA embedding both in clinical medicine and in animal experimental studies of undecalcified bone samples.

Correspondence to: Dr. Antonio Nanci, Université de Montréal, Faculty of Dentistry, Dept. of Stomatology, PO Box 6128, Station Centre-Ville, Montreal, QC, Canada H3C 3J7. E-mail: Antonio.Nanci@UMontreal.CA

Received for publication June 5, 2002; accepted September 18, 2002 (2A5827).

The glycolated form of methacrylate (glycolmethacrylate, GMA) is employed for both light and electron microscopic immunolabeling. GMA is a bifunctional methacrylate that forms crosslinks during polymerization. Consequently, it cannot be dissolved out of sections (Wolf et al. 1992), limiting its application for conventional histomorphometric analyses. This is not the case for MMA. However, this resin has been mainly used for light microscopic immunolabeling, and its application in electron microscopy is not well documented (Baskin et al. 1992). Therefore, the aim of the present study was to investigate whether MMA embedding can be used for ultrastructural immunolabeling of two predominant bone matrix proteins, bone sialoprotein (BSP) and osteopontin (OPN), and to compare the results with those obtained with LR White (LRW) resin, under tissue processing conditions conventionally used with these resins. The latter acrylic-based resin allows good performance in immunocytochemistry (Bendayan et al. 1987) and has been used for cytochemical characterization of the presence and distribution of noncollagenous matrix

proteins in calcified tissues (Nanci et al. 1989; McKee and Nanci 1995). The results indicate that MMA is applicable to the ultrastructural immunolocalization of BSP and OPN in bone matrices.

Materials and Methods

Tissue Processing

Male Wistar rats weighing 100 ± 10 g (Charles River Canada; St-Constant, QC, Canada) were anesthetized with chloral hydrate (0.4 mg/g body weight). For embedding in LRW (London Resin Company; Berkshire, UK), rats were perfused for 20 min with a mixture of 4% paraformaldehyde and 0.1% glutaraldehyde in 0.1 M phosphate buffer, pH 7.2, and tibiae were dissected out, cut in half along their length, and immersed in the same fixative overnight. The samples were dehydrated in graded ethanol and then embedded in resin that was polymerized at 58°C for 48 hr, as described previously (Nanci et al. 1989). For embedding in MMA (J-T Baker; Phillipsburg, NJ), just after anesthesia, tibiae were dissected, split in half, placed directly in ethanol, and subsequently impregnated with a MMA mixture. Briefly, samples were infiltrated for 4 days at 4°C in a clear glass scintillation vial containing a mixture of 80% (v/v) MMA, 20% (v/v) *N*-dibutylphthalate, and 3.4% (weight) benzoyl peroxide. They were then placed in fresh MMA and at 32°C for 3–4 days until the resin hardened. Procedures for animal handling and perfusion have been approved by le Comité de Déontologie de l'Université de Montréal.

For light microscopy, semithin sections ($1 \mu\text{m}$) of the primary spongiosa were cut with a glass knife on a Reichert Ultracut E microtome and stained with toluidine blue or by the von Kossa method. Thin sections of regions near the center of the growth plate were then prepared with a diamond knife, mounted on Formvar-carbon-coated nickel grids, and processed for postembedding protein A-gold immunocytochemistry (reviewed in Bendayan 1995).

Immunolabeling for BSP and OPN

Grid-mounted tissue sections of LRW- and MMA-embedded undecalcified bone were floated for 15 min on a drop of 0.01 M PBS containing 1% ovalbumin (Oval; Sigma Chemical, St Louis, MO) to saturate nonspecific binding sites, and then were transferred to and incubated for 3 hr on a drop of polyclonal chicken egg yolk anti-rat OPN antibody (Nanci et al. 1996) diluted 1:150 with PBS. After incubation, sections were rinsed with PBS, placed on PBS-Oval for 15 min, and then transferred for 1 hr onto a drop of rabbit anti-chicken IgG (Cappel Research Products; Scarborough, ON, Canada), diluted 1:2000 with PBS. Finally, they were rinsed with PBS, placed on PBS-Oval for 15 min, and incubated for 30 min with protein A-gold complex (8–10 nm diameter) prepared in house according to Bendayan (1995). Other grid-mounted sections were blocked with PBS-Oval and incubated for 1 hr on a drop of polyclonal anti-rat BSP antibody (diluted 1:10 with PBS; the LF87 was courtesy of Dr. L.W. Fisher, National Institutes of Health, Bethesda, MD; Fisher et al. 1995). In the latter case no secondary antibody was used and grids were washed, blocked, and directly incubated with the protein A-gold complex. As controls, sec-

tions were incubated with protein A-gold alone. All incubations were performed at room temperature in a moist environment. The grids were then washed thoroughly with PBS, rinsed with distilled water, and air-dried. All sections were routinely stained with uranyl acetate and lead citrate and examined using a JEOL JEM 1200EX II transmission electron microscope operated at 60 kV.

Quantitative Analysis of the Immunolabeling

Images were printed at a final magnification of $\times 38,000$ and digitized using a Sony CCD 7002P camera (Sony Corporation; Tokyo, Japan). The number of gold particles per print, over interfibrillar accumulations of noncollagenous matrix (patches), and over collagenous regions of bone was quantified and compared using a Q500 image analysis system (Leica; Cambridge, UK). Based on the fact that NCPs accumulate mainly as interfibrillar patches (reviewed in Nanci 1999), a morphometric program was set up to recognize and measure the area of regions in which there was a concentration of gold particles, as determined by a threshold distance between particles. For each print, a visual control by the same operator was made to ensure that the regions selected did indeed correspond to interfibrillar areas. For statistical analyses, Systat version 10 software (SPSS; Chicago, IL) was used. Because the data did not show a normal distribution, the number of particles obtained after incubation of MMA and LRW sections with BSP or OPN was compared using the Mann-Whitney *U*-test. For the labeling over patches, a two-sample *t*-test with separate variances was used. Three categories of photographic fields were arbitrary defined based on number of patches/ $20 \mu\text{m}^2$; less than 8, 8 to 16 and greater than 17. The Pearson chi-square test was used to compare the

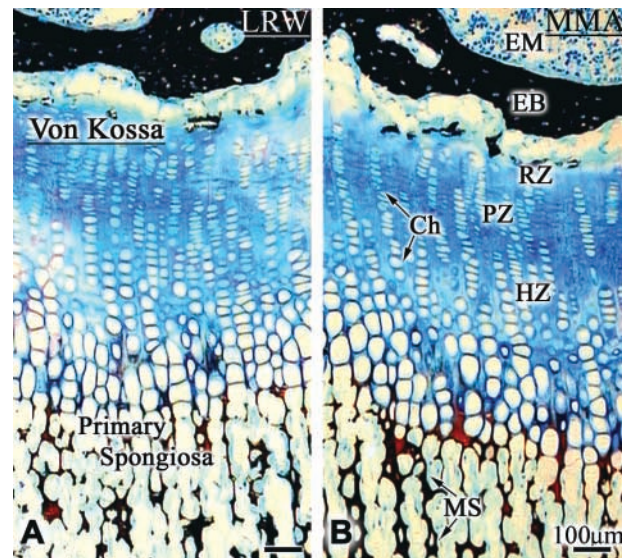


Figure 1 Endochondral ossification in rat tibia. (A) LR White (LRW) and (B) methylmethacrylate (MMA) sections of nondecalcified tibiae stained by the von Kossa method and counterstained with toluidine blue. Structural appearance and staining are similar with both resins. Ch, chondrocytes; EB, epiphyseal bone; EM, epiphyseal marrow; HZ, hypertrophic zone; MS, mixed spicules; PZ, proliferation zone; RZ, resting zone.

two resins for distribution of patches within each category. The relationship between labeling density and the number of patches was evaluated by linear regression (Pearson correlation). For the number of particles and the proportion of labeling within patches, PASS 6.0 software (Dynalab; Reynoldsburg, OH) was used to determine power (alpha level = 0.05) and the smallest difference between groups that would allow a power of 0.80 at the alpha level of 0.05.

Results

Structural Features

Von Kossa staining did not reveal any difference in the staining pattern and intensity observed over bone and calcified cartilage embedded in MMA or LRW (Figures 1A and 1B). Ultrastructural preservation was generally better and more consistent with LRW processing, but MMA processing also permitted visualization of cellular features in some regions (compare Figures 2A and 2B). Likewise, there was no significant difference in the appearance of the matrix (compare Figures 3A and 3B, and Figures 3C and 3D).

Immunolocalization of BSP and OPN

The distribution of immunolabeling for BSP and OPN was similar for MMA- and LRW-embedded speci-

mens. With both resins, gold particles were found mainly over the calcified bone matrix; some were also seen over osteoid. The labeling was mostly associated with electron-dense portions of the matrix, i.e., over cement lines and interfibrillar accumulations (patches) of granular/reticular-textured organic matrix (Figure 3). Incubation of tissue sections with protein A-gold alone resulted in the occasional presence of particles throughout sections.

Quantitative Analysis of the Immunolabeling

Numerical parameters for the number of gold particles obtained after incubation of tissue sections with BSP and OPN antibodies are summarized in Table 1. For both BSP and OPN incubations, the distribution of patches/surface area within the three arbitrarily defined density categories was comparable for bone samples embedded in either MMA or LRW. For both resins, about 44% of the bone surface examined fell within the 8–16 patches/20 μm^2 category and nearly 28% in the >17 patches category (Figure 4). With both antibodies, there was no significant difference in mean numbers of total gold particles/micrograph observed over the two resins (Figure 5A). Power analysis indicated that the number of samples studied was suf-

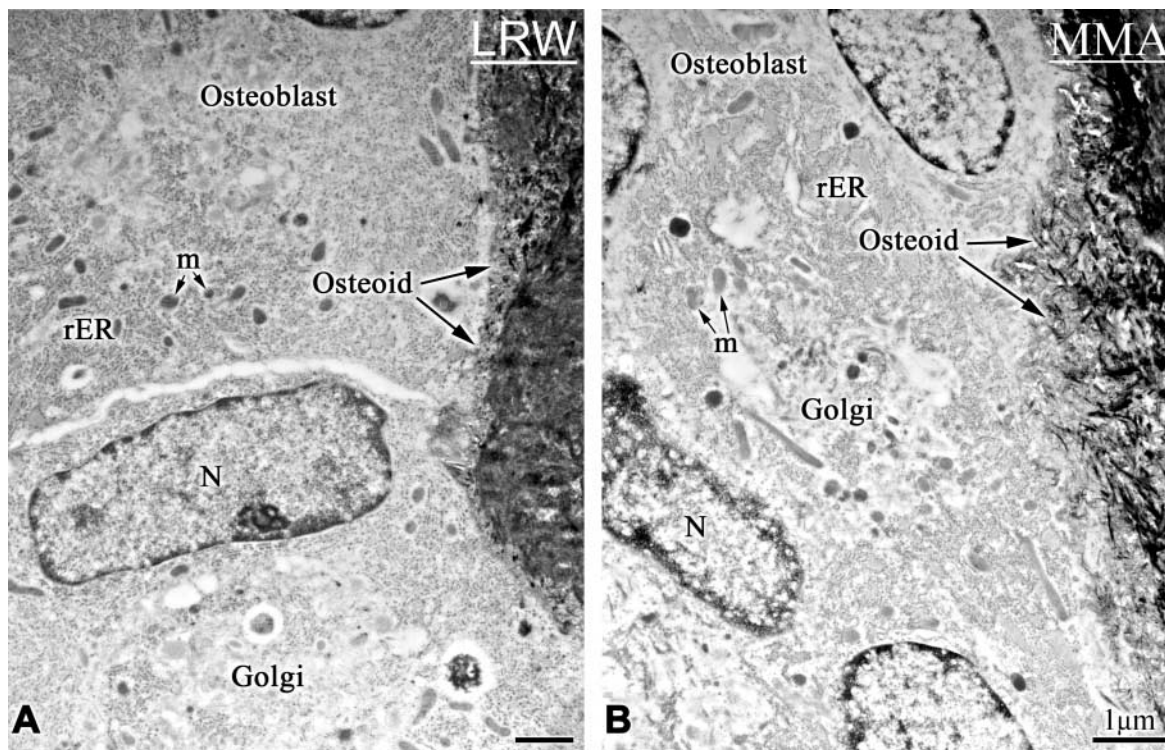


Figure 2 Electron micrographs from the primary spongiosa of rat tibiae, illustrating the ultrastructural preservation in (A) LR White (LRW)- and (B) in better-preserved regions of methylmethacrylate (MMA)-embedded samples. Osteoblasts are apposed to osteoid and exhibit cytoplasmic features of cells actively involved in protein secretion. The rough endoplasmic reticulum (rER) is extensive and the Golgi apparatus is well developed. m, mitochondria; N, nucleus.

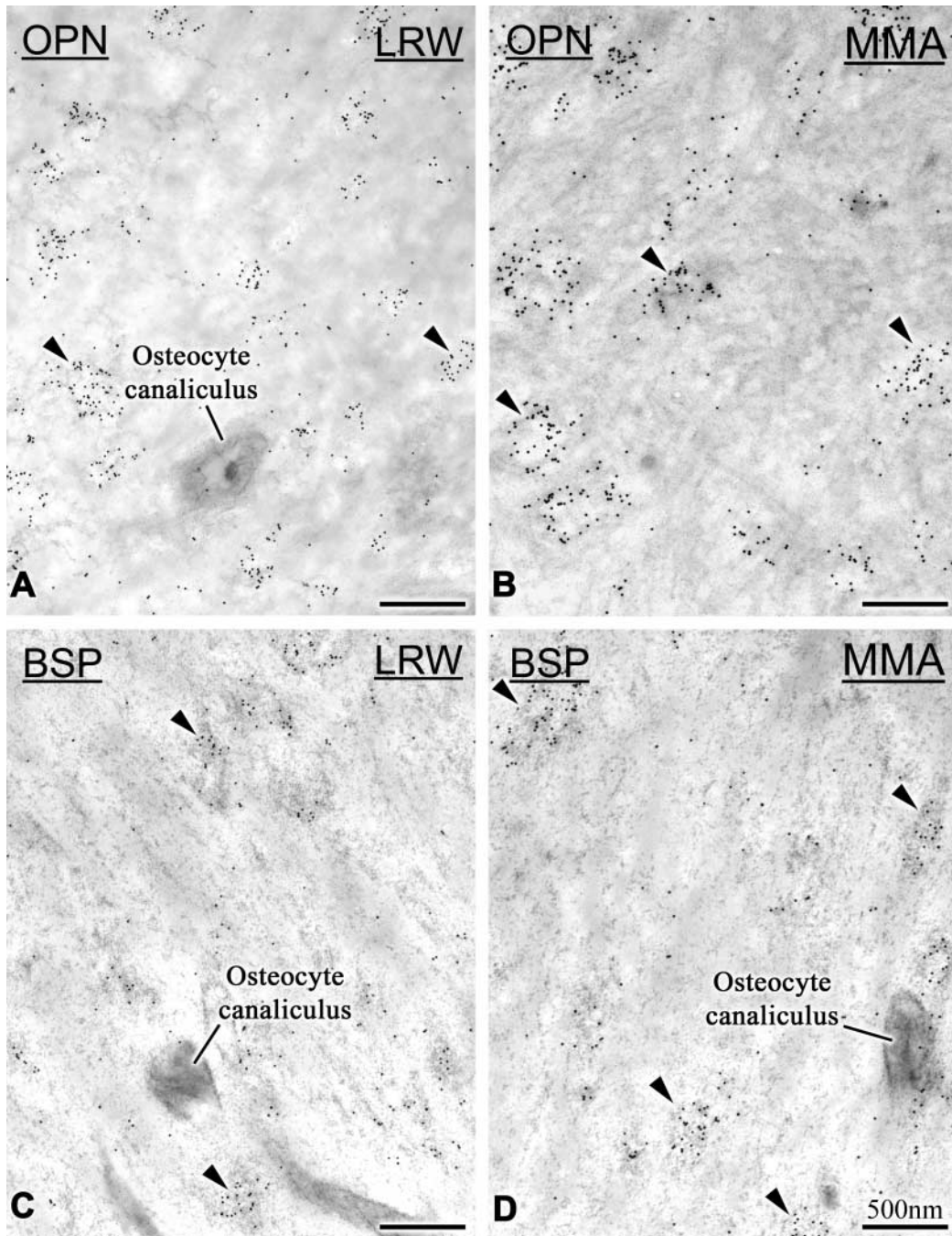


Figure 3 Immunocytochemical preparations with anti-rat osteopontin (OPN) and anti-rat bone sialoprotein (BSP) antibodies. (A,C) LR White (LRW)-embedded tibiae; (B,D) methylmethacrylate (MMA) tibiae. The bone matrix shows a similar structural appearance with both resins. With both resins, immunoreactivity for BSP and OPN co-localizes and gold particles are mainly found over interfibrillar patches of granular/reticular-textured organic matrix (arrowheads).

ficient to allow an 80% chance of detecting a difference of 102.2 particles for BSP and 109.6 particles for OPN at a 0.05 level of statistical significance.

The majority of the immunolabeling was found over the patches, and there was no significant differ-

ence in labeling density over them between the two resins (Figure 5B). Patches represented an average of 19% of the observed bone surfaces but an average of 88% of the labeling was found over them (Table 1). The relationship between labeling density and the

Table 1 Quantitative analysis of immunolabeling over LR White- and methylmethacrylate-embedded bone^a

	Antibody	Resin		Mann-Whitney <i>U</i> -test	Two-sample <i>t</i> -test value	Difference for power = 0.80
		LRW	MMA			
Range in particle counts	BSP	283–792	319–864			
	OPN	337–1011	332–923			
Median no. particles	BSP	438	456	580.0 ($p=0.56$)		102.2
	OPN	577	496	792.0 ($p=0.06$)		109.6
% area occupied by NCP accumulations (patches)	BSP	18.5	21.5			
	OPN	16.8	18.2			
No. patches per field \pm SD	BSP	11.2 \pm 5.9	11.6 \pm 5.1		-0.24 ($p=0.81$)	4.3
	OPN	14.9 \pm 5.8	13.1 \pm 5.8		1.20 ($p=0.23$)	4.2
% particles over patches	BSP	87.0 \pm 1.7	85.2 \pm 0.8	$U=477.0$ ($p=0.092$)	0.95 ($p=0.35$)	5.3
	OPN	90.8 \pm 0.7	89.0 \pm 0.8	$U=610.0$ ($p=0.068$)	1.71 ($p=0.09$)	3.0

^aBSP, bone sialoprotein; LRW, LR White resin; MMA, methylmethacrylate; OPN, osteopontin.

number of patches was linear for both BSP and OPN (Figure 6).

The mean number per area of gold particles obtained with both BSP and OPN over osteoid was 4.3 for MMA and 6.25 for LRW, over nuclei 2.5 and 3.5, respectively, and over cartilage 0 and 0.44, respectively (data not shown).

Discussion

Whereas MMA is widely used for histomorphometric analysis of bone biopsy specimens, (Theuns et al. 1993), its application for immunolabeling has been limited. Indeed, it is generally believed that the high temperature generated by reactive radicals during polymerization of the resin is not compatible with retention of antigenic determinants (Cole 1982; Ashford et al. 1986; Baskin et al. 1992; Wolf et al. 1992; Erben 1997). Nevertheless, the use of conventional processing yielded inconsistent and suboptimal cell preverva-

tion, and distribution of immunolabeling and density were similar to those obtained with LRW, a resin polymerized at 58C. It has been determined that the maximal temperature reached by MMA when polymerized at room temperature does not exceed 60C (Theuns et al. 1993). Therefore, when polymerized at 32C, as in the present case, it is likely to go above this temperature. However, compared with LRW, the MMA embedding procedure does not significantly alter antigenic properties, at least for BSP and OPN, and the temperature generated during polymerization certainly does not dramatically affect antigenicity of typical noncollagenous matrix proteins in calcified bone. This may be due to the fact that these proteins are intimately associated with the mineral phase, which may prevent their denaturation. However, lower temperatures may, however, be important for more labile antigens such as cell proteins and enzymes.

The labeling for BSP and OPN, respectively, obtained with undecalcified sections of MMA- and LRW-embedded bone (fixed as conventionally used with these resins) shows similar distributions and densities. In addition, the BSP:OPN labeling density ratios are essentially similar, indicating that MMA and LRW affect the antigenic properties of both BSP and OPN in a similar manner.

Matrix organization and relative proportions of collagenous and noncollagenous components in bone represent important parameters that vary with development stage and anatomic site, and reflect local tissue dynamics (Bianco 1992; Nanci 1999). In the region of the rat primary spongiosa examined, interfibrillar accumulations of noncollagenous matrix proteins occupy 16–21% of the bone surface area, and 85–90% of the BSP or OPN immunolabeling is found over them. The observed variability in density of noncollagenous matrix protein patches within photographic fields is likely associated with microanatomic

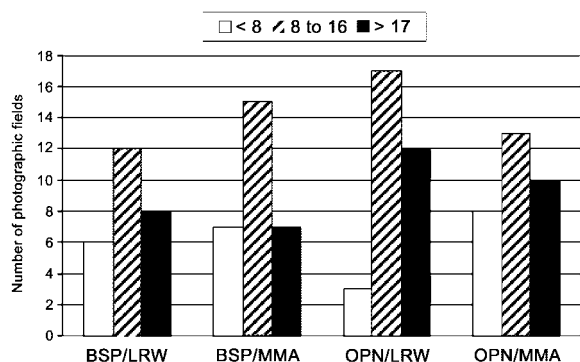


Figure 4 Classification of bone surfaces according to frequency of noncollagenous matrix patches. Nearly half of the surfaces contain 8–16 patches/20 μm².

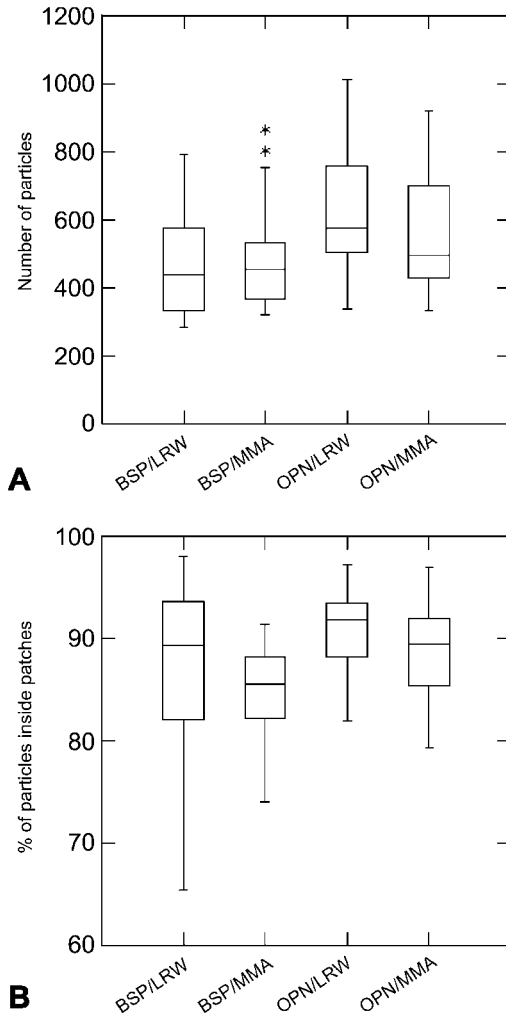


Figure 5 Box plots comparing structural and immunocytochemical parameters in LR White (LRW) and methylmethacrylate (MMA). **(A)** Total number of gold particles per micrograph observed after incubation with anti-bone sialoprotein (BSP) and anti-osteopontin (OPN) over the two resins. There is no statistical difference in particle counts between LRW and MMA. **(B)** Percentage of gold particles found over patches. The majority of immunolabeling (>80%) is over interfibrillar matrix. Asterisks, outside value.

variations in the relative proportions of the collagenous and noncollagenous components. In this context, it has been proposed that the amount of interfibrillar matrix depends on the packing density of collagen which is, in part, determined by the speed at which it is deposited (discussed in Nanci 1999; Bosshardt and Nanci 2000).

Although the number of gold particles over cartilage was almost nonexistent with both resins, osteoid showed roughly twice as many particles as over nuclei. Labeling over nuclei is used as an indication of background (Bendayan 1995). The presence of a higher

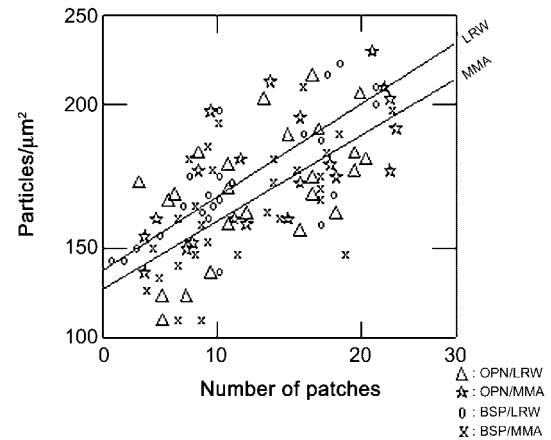


Figure 6 Both resins show a linear relationship between the density of gold particles and the number of patches ($p < 0.001$). The square multiple r^2 value indicates that the variability in gold particle density can be explained by the frequency of accumulations (patches) of noncollagenous matrix proteins.

number of gold particles over osteoid, albeit at a very low density, is consistent with a diffusion of secreted molecules from the osteoblast surface towards the mineralization front; a similar observation has been made for osteocalcin (Camarda et al. 1987).

In conclusion, our study shows that it is possible to detect and immunolocalize BSP and OPN in sections of alcohol-fixed rat bone embedded in MMA from which the resin is not removed. This finding is important because it highlights the feasibility of processing experimental and clinical bone samples for parallel light microscopic and histomorphometric analyses, and for compositional studies at the ultrastructural level. In addition, it offers the possibility to further exploit valuable MMA-embedded bone samples from previous studies by determining whether the morphological and histomorphometric alterations observed are associated with changes in the content and/or distribution of major matrix proteins.

Acknowledgments

Supported by the Canadian Institutes of Health Research. We are grateful to Natalie Dion (Hôpital St Luc, Montréal) for MMA embedding, Sylvia Zalzal (Université de Montréal) for advice with immunolabeling, Micheline Fortin (Université de Montréal) for assistance with tissue sectioning, Pierre Rompré (Université de Montréal) for statistical analysis, and Paul Pilet (Inserm 99-03, Nantes) for adapting the gold particle counting software.

Literature Cited

Ashford AE, Allaway WG, Gubler F, Lennon A, Slegers J (1986) Temperature control in Lowicryl K4M and glycol methacrylate during polymerization: is there a low-temperature embedding method? *J Microsc* 144:107-126

- Baskin TI, Busby CH, Fowke LC, Sammut M, Gubler F (1992) Improvements in immunostaining samples embedded in methacrylate: localization of microtubules and other antigens throughout developing organs in plants of diverse taxa. *Planta* 187:405–413
- Bendayan M (1995) Colloidal gold post-embedding immunocytochemistry. *Prog Histochem Cytochem* 29:1–159
- Bendayan M, Nanci A, Kan FW (1987) Effect of tissue processing on colloidal gold cytochemistry. *J Histochem Cytochem* 35:983–996
- Bianco P (1992) Structure and mineralization of bone. In Bonucci E, ed. *Calcification in Biological Systems*. Boca Raton, FL, CRC Press, 243–268
- Bosshardt DD, Nanci A (2000) The pattern of expression of collagen determines the concentration and distribution of noncollagenous proteins along the forming root. In Goldberg M, Boskey A, Robinson C, eds. *Chemistry and Biology of Mineralized Tissues*. Rosemont, IL, American Academy of Orthopaedic Surgeons, 129–136
- Camarda AJ, Butler WT, Finkelman RD, Nanci A (1987) Immunocytochemical localization of gamma-carboxyglutamic acid-containing proteins (osteocalcin) in rat bone and dentin. *Calcif Tissue Int* 40:349–355
- Cole MB Jr (1982) Glycol methacrylate embedding of bone and cartilage for light microscopic staining. *J Microsc* 127:139–148
- Derkx P, Nigg AL, Bosman FT, Birkenhäger-Frenkel DH, Houtsmuller AB, Pols HAP, Van Leeuwen JPT (1998) Immunolocalization and quantification of noncollagenous bone matrix proteins in methylmethacrylate-embedded adult human bone in combination with histomorphometry. *Bone* 22:367–373
- Erben RG (1997) Embedding of bone samples in methylmethacrylate: an improved method suitable for bone histomorphometry, histochemistry, and immunohistochemistry. *J Histochem Cytochem* 40:307–313
- Fisher LW, Stubbs JT, Young MF (1995) Antisera and cDNA probes to human and certain animal model bone matrix noncollagenous proteins. *Acta Orthop Scand* 66:61–65
- Gruber HE, Marshall GJ, Kirchen ME, Kang J, Massry SG (1985) Improvements in dehydration and cement line staining for methacrylate embedded human bone biopsies. *Stain Technol* 60:337–344
- McKee MD, Nanci A (1995) Postembedding colloidal-gold immunocytochemistry of noncollagenous extracellular matrix proteins in mineralized tissues. *Microsc Res Tech* 31:44–62
- Nanci A (1999) Content and distribution of noncollagenous matrix proteins in bone and cementum: relationship to speed of formation and collagen packing density. *J Struct Biol* 126:256–269
- Nanci A, Ahluwalia JP, Zalzal S, Smith CE (1989) Cytochemical and biochemical characterization of glycoproteins in forming and maturing enamel of the rat incisor. *J Histochem Cytochem* 37:1619–1633
- Nanci A, Zalzal S, Gotoh Y, McKee MD (1996) Ultrastructural characterization and immunolocalization of osteopontin in rat calvarial osteoblast primary cultures. *Microsc Res Tech* 33:214–231
- Theuns HM, Bekker H, Fokkenrood H, Offerman E (1993) Methylmethacrylate embedding of undecalcified rat bone and simultaneous staining for alkaline and tartrate resistant acid phosphatase. *Bone* 14:545–550
- Wolf E, Röser K, Hahn M, Welkerling H, Delling G (1992) Enzyme and immunohistochemistry on undecalcified bone and bone marrow biopsies after embedding in plastic: a new embedding method for routine application. *Virchows Arch [A] Pathol Anat Histopathol* 420:17–24